Estimation of mean exocytic vesicle capacitance in mouse adrenal chromaffin cells

(exocytosis/synaptic-like microvesicles/amperometry/membrane capacitance/noise analysis)

TOBIAS MOSER AND ERWIN NEHER

Department of Membrane Biophysics, Max Planck Institute for Biophysical Chemistry, Am Fassberg, D-37077, Germany

ABSTRACT Whole-cell membrane capacitance measurements are frequently used to monitor neuronal and nonneuronal secretory activity. However, unless individual fusion events can be resolved, the type of the fusing vesicles cannot be identified in these experiments. Here we apply statistical analysis of trial-to-trial variations between depolarization-induced capacitance increases of mouse adrenal chromaffin cells and obtain estimates for the capacitance contribution of individual exocytic vesicles between 0.6 and 2 fF. For comparison, measurements of membrane capacitance were combined with amperometric recordings of catecholamine release during intracellular perfusion of chromaffin cells with high $[Ca^{2+}]$. Crosscorrelation of both signals yielded a mean capacitance contribution of individual catecholaminergic vesicles of 1.3 fF. We suggest that depolarization-induced capacitance increases in mouse adrenal chromaffin cells mainly represent fusion of chromaffin granules.

Measurements of membrane capacitance (C_m) are used to study Ca^{2+}-regulated exocytosis with high time resolution (reviewed in refs. 1 and 2). In many cases the vesicles are too small to be resolved as individual fusion events in whole-cell capacitance recordings. This is true also for chromaffin granules (3, 4) and even more for small synaptic-like microvesicles (SLMVs), which are present in neuroendocrine cells (reviewed in ref. 5). Capacitance recordings from single chromaffin cells in mouse adrenal slices have revealed a very fast exocytic component in response to membrane depolarization (ref. 6, time constant 7 ms). Does this fast C_m rise represent fusion of chromaffin granules, SMLVs, or both? The uncertainty about the type of small fusing vesicles is circumvented if the release itself can be independently detected, for example by amperometry (7, 8), provided that only one vesicle type contains oxidizable substances. However, recently catecholamine storage was suggested not only for chromaffin granules but also for SLMVs in chromaffin cells (9). Moreover, in contrast to C_m measurements, the carbon-fiber microelectrodes detect release only from a variable portion of the cell. Thus, if exocytosis preferentially takes place at certain regions of the plasma membrane, the amperometrically detected release might not be representative for the secretion of the whole cell. Therefore, even combined C_m and amperometric measurements do not necessarily answer the question of how many vesicles of which kind are released during a secretory response.

We stimulated secretion in isolated mouse chromaffin cells by intracellular perfusion with high $[Ca^{2+}]$ and observed only one population of catecholaminergic vesicles in amperometric recordings, most likely chromaffin granules. Averaging of the simultaneously recorded C_m traces—time-locked at the peak of amperometric spikes—revealed corresponding C_m step increases similar to the mean single-vesicle capacitance estimated from fluctuations in depolarization-induced capacitance increases in mouse chromaffin cells in slices. From this comparison we conclude that the fast secretory component in mouse chromaffin cells in slices mainly represents release of chromaffin granules.

MATERIALS AND METHODS

Adrenal Slice Preparation and Preparation of Isolated Chromaffin Cells. Adrenal glands from adult female NMRI mice were used. Slices (170 to 250 μm thick) were prepared following standard slicing procedures (10). Details are given elsewhere (6). Slices were used starting shortly after cutting for 6 to 10 hr. Cell isolation and primary culture have been described before (6). In brief, collagenase A (Boehringer Mannheim) was used at a concentration of approximately 3 units/ml (in Locke's buffer) for digestion of the minced tissue. Cells were plated in M199 culture medium (including penicillin/streptomycin, 10% fetal calf serum, and 1 mg/ml albumin) on poly-L-lysine-coated coverslips. Cells were used for experiments from the day of culture through day 2 after culture.

Whole-Cell Patch-Clamp and Capacitance Measurements. Conventional whole-cell recordings (11) were performed with Sylgard-coated 3- to 4-MΩ (slice) or 2- to 3-MΩ (isolated cells) pipettes. Series resistances ranged from 5 to 12 MΩ. An EPC-9 patch-clamp amplifier was used together with PULSE software (HEKA Elektronics, Lambrecht, Germany). Capacitance measurements were performed using the Lindau–Neher technique implemented as the "sine+dc" mode of the software lock-in extension of PULSE software. A 1-kHz, 70-mV (depolarization experiments) or 100-mV (crosscorrelation) peak-to-peak sinusoid stimulus was applied about a dc holding potential of −80 mV. Electrical coupling of chromaffin cells in slices was not a major problem because of the low coupling conductance (<500 pS; T.M., unpublished observation) and the high sinewave frequency. Currents were filtered at 2 kHz and sampled at 12 kHz. Slices were bathed in a bicarbonate-buffered saline (external solution 1: 125 mM NaCl/26 mM $NaHCO_3$/2.5 mM KCl/1.25 mM NaH_2PO_4/2 mM $CaCl_2$/1 mM $MgCl_2$/10 mM glucose/0.2 mM *d*-tubocurarine, bubbled with 95% O_2/5% CO_2, pH 7.4, perfusion at 1 to 2 ml/min). The pipette solution (internal solution 1) contained 145 mM Cs-glutamate, 8 mM NaCl, 1 mM $MgCl_2$, 2 mM Mg-ATP, 0.3 mM Na_2-GTP (Boehringer Mannheim), and 10 mM Cs-Hepes, and its $[Ca^{2+}]_{free}$ was adjusted at 300 nM by mixing Ca^{2+} loaded and free EGTA (K_d: 150 nM, total EGTA 300 μM). The bathing solution (external solution 2) for isolated cells contained 150 mM NaCl, 2.8 mM KCl, 10 mM $CaCl_2$, 1 mM $MgCl_2$, 10 mM Na-Hepes, and 0.2 mM *d*-tubocurarine (pH 7.2). The pipette solution (internal solution 2) contained 145 mM Cs-glutamate, 8 mM NaCl, 2 mM HEDTA, 1.5 mM $MgCl_2$, 1.5 mM $CaCl_2$, 2 mM Mg-ATP, 0.3 mM Na_2-GTP, 10 mM

Abbreviations: C_m, membrane capacitance; SLMV, synaptic-like microvesicles.

Cs-Hepes ($[Ca^{2+}]_{free}$: $\approx$10 μM). Chemicals were from Sigma unless stated otherwise.

Amperometry. Electrodes were prepared as described in ref. 12 from 10-μm thick carbon fibers (Amoco Performance Products, Greenville, SC) and were fitted into patch pipette holders with the fibers canulated through glass capillaries. A constant voltage of 650 mV vs. Ag/AgCl was applied to the electrode, whose cross-sectional (tip) surface was gently pressed against the cell surface. The amperometric current was filtered at 1 kHz and sampled at 12 kHz.

Data Analysis and Theory. Analysis was performed using Igor software (WaveMetrics, Lake Oswego, OR). Data are given as mean $\pm$ SEM unless stated otherwise. For our statistical analysis we consider trial-to-trial variations of capacitance increases during repetitive depolarizing stimulation in analogy to the ensemble noise analysis of Sigworth (13). We assume that the capacitance change (ΔC_m) in response to a given depolarization represents a sum of exocytic capacitance increments and a constant nonsecretory C_m artifact (ΔC_t) due to sodium channel gating charge movement (transient in Fig. 2A; refs. 6 and 14). Our initial hypothesis is that the exocytic capacitance increments are due to fusion of only one type of vesicles, whose mean vesicle capacitance is Δc. For a trial we expect:

$$\Delta C_m = x_i \Delta c + \Delta C_t, \qquad [1]$$

where x_i is the number of fused vesicles at this trial. We assume that the number of fusing x_i vesicles follows a Poisson distribution with the parameter λ (number of release sites $\times$ release probability) under stationary conditions (constant λ). The mean $\langle \Delta C_m \rangle$ is given by:

$$\langle \Delta C_m \rangle = \lambda \Delta c + \langle \Delta C_t \rangle, \qquad [2]$$

and the variance $\sigma^2_{\Delta C_m}$ by:

$$\sigma^2_{\Delta C_m} = \lambda \Delta c^2 + \sigma^2_t. \qquad [3]$$

If λ is not constant but varies slowly, variance can be evaluated over sufficiently short segments of data and a plot of measured variances versus their corresponding means is expected to result in a straight line according to Δc. From Eqs. **2** and **3** we derive:

$$\sigma^2_{\Delta C_m} = \Delta c (\langle \Delta C_m \rangle - \langle \Delta C_t \rangle) + \sigma^2_t \qquad [4]$$

differentiation of Eq. **4** with respect to $\langle \Delta C_m \rangle$ directly yields Δc:

$$\frac{\delta \sigma^2_{\Delta C_m}}{\delta \langle \Delta C_m \rangle} = \Delta c. \qquad [5]$$

In whole-cell recordings from chromaffin cells rundown of the secretory response with increasing experimental time was observed (6, 15, 16). Variances and means were calculated for groups with n of 4 to 8 neighboring ΔC_m values during which the change in λ was small. The analysis window ΔC_m was moved point by point, which in many experiments displayed a monotonic drop of λ. Sample mean (M) and sample variance (S^2) over the n ΔC_m values in a window were evaluated as:

$$M = \frac{1}{n} \sum \Delta C_{mi} \qquad [6]$$

and

$$S^2 = \frac{1}{(n-1)} \sum_{i=1}^{n} (\Delta C_{mi} - M)^2. \qquad [7]$$
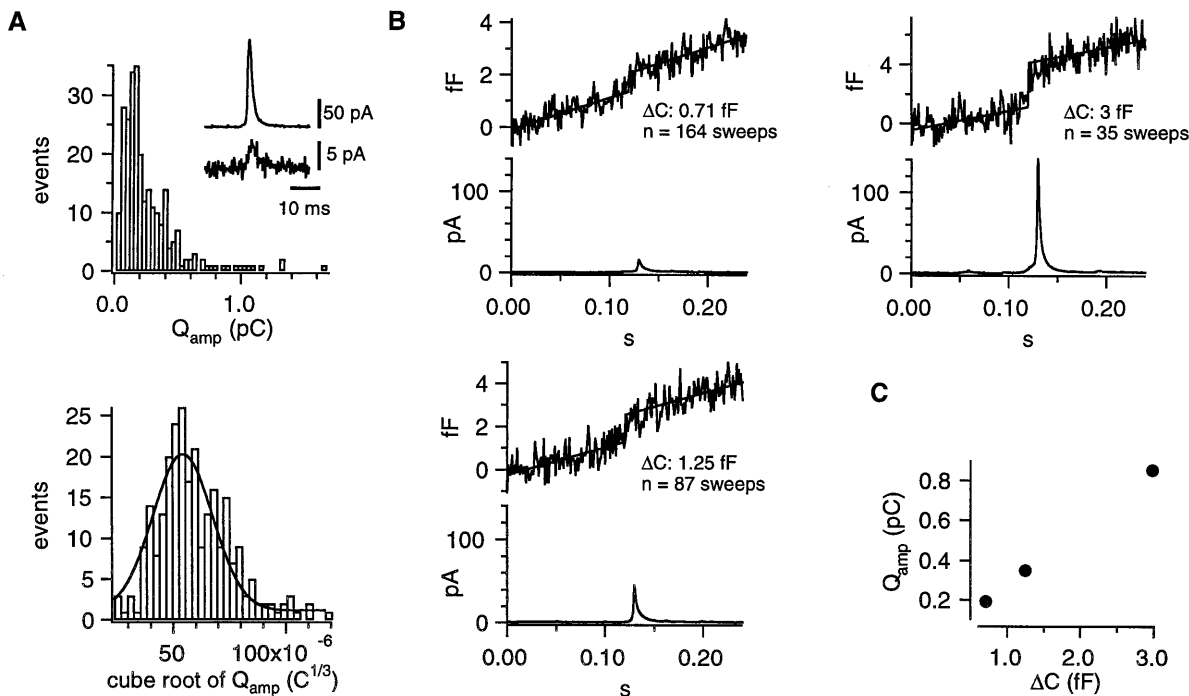

Fig. 1.   Analysis of amperometric spikes and single vesicle capacitance during secretion of isolated chromaffin cells. Cells were stimulated by intracellular perfusion with high $[Ca^{2+}]$ (internal solution 2) and bathed in Ringer's solution (external solution 2). (A) The top graph shows the distribution of the current integrals (Q_{amp}) of the fastest amperometric spikes (risetime <1.5 ms). The *Inset* displays the smallest fast spike (peak amplitude $\approx$4 pA) detected and compares it it to a large one, recorded during the same experiment. The lower graph displays the $\sqrt[3]{Q_{amp}}$ histogram. A Gaussian fit (solid line) is superimposed. Its mean and SD were 54.2×10^{-6} and 18.7×10^{-6} $C^{1/3}$, respectively. (B) Time-locked ΔC_m (*Upper*) and amperometric current (*Lower*) averages for three groups. Top, left: spikes <23 pA; bottom, left: spikes >23 pA but <70 pA; right, top: spikes >70 pA. The Δc values were estimated as the y $-$ difference of two parallel lines fitted to the average trace (up to 20 ms before the spike-peak, and from 20 ms after the spike-peak). (C) Plot of the Q_{amp} of the average spikes versus Δc.

Biophysics: Moser and Neher

Proc. Natl. Acad. Sci. USA 94 (1997)   6737

Values of S^2 were plotted against M values and Δc was estimated according to Eq. **5** as the slope of a linear regression to such a plot.

RESULTS

Amperometric Spike Parameters and Capacitance of Single Catecholaminergic Vesicles Released During Intracellular Perfusion with High [Ca²⁺]. Intracellular perfusion with high [Ca^{2+}] ($\approx 10\ \mu M$, internal solution 2) via the patch-pipette was used to stimulate robust, long-lasting catecholamine secretion in isolated mouse chromaffin cells. Whole-cell capacitance and the amperometric current of an attached carbon-fiber electrode were simultaneously recorded. Only release events occurring close to the detector were considered (30/90% rise time <1.5 ms). The smallest fast spike detected had an amplitude of ≈ 4 pA (see insert of Fig. 1*A*). Amplitude and halfwidth of the amperometric spikes had medians ($\pm SE$) of 27.0 ± 2.2 pA and 3.6 ± 0.1 ms, respectively. Fig. 1*A* shows that the integrals of the amperometric current spikes (Q_{amp}, representing the detected amount of oxidizable molecules released from a vesicle, top) followed a skewed distribution whereas the cube-roots of the integrals ($\sqrt[3]{Q_{amp}}$), proportional to the vesicle diameter in case of a constant concentration, bottom) were much closer to a normal distribution. In contrast to serotoninergic and dopaminergic neurons (17, 18), which release two populations of monoamine-containing vesicles, there was no peak or shoulder at low Q_{amp} of the Q_{amp} histogram in chromaffin cells. The relative SD of $\sqrt[3]{Q_{amp}}$ (0.34, taken from the Gaussian fit to the data) was similar to that observed for chromaffin granule sizes in an ultramorphological study (0.39, taken from an Gaussian fit to the diameter distribution of isolated rat chromaffin granules of table 6 in ref. 19). We conclude that we detected only one population of catecholaminergic vesicles—that of chromaffin granules. Therefore, if catecholaminergic SLMVs are present in chromaffin cells—as reported by a recent biochemical study (9)—they seem not to be released during stimulation with elevated intracellular [Ca^{2+}] up to 10 μM or else their contribution to the amperometric current is so small that unitary events cannot be resolved.

To obtain estimates for the capacitance of individual vesicles of different sizes a time-locked signal averaging (4) was applied to the C_m traces because individual chromaffin granule fusion cannot be resolved in whole-cell C_m measurements. The peak location of amperometric spikes was used to align segments of the simultaneously recorded C_m data before averaging. According to the spike amplitude the amperometric signals and the corresponding C_m traces were grouped in small (<23 pA), medium (>23 pA but <70 pA), and large (>70 pA) events. Only spikes with halfwidths shorter than 15 ms were considered. Data of 10 cells were analyzed. Fig. 1*B* shows the averages of both the amperometric and the C_m signals. In all three groups capacitance step increases (Δc) were obtained, whereas randomly aligned C_m traces did not show such steps (data not shown). The Q_{amp} values of the average spikes and the corresponding Δc were positively correlated (Fig. 1*C*). The numbers of averaged traces in Fig. 1 indicate that small and medium-size spikes occurred more frequently than large ones during intracellular perfusion with high [Ca^{2+}]. Ungrouped crosscorrelation—similar to (4), but also considering broader spikes—was performed individually for nine cells. The average Δc was 1.28 ± 0.15 fF.

Estimation of the Mean Δc of Vesicles Fused upon Depolarization. The main objective of the present study was to clarify which types of vesicles fuse during the fast depolarization-induced secretory component of chromaffin cells in slices. Unfortunately, the amperometric approach proved difficult in slices (spill-over of catecholamines, diffusion-delayed spikes). In addition to the technical problem, we were motivated to use

a mean Δc estimation solely based on capacitance measurements because that should reflect exocytosed vesicles regardless of their content. A mean Δc estimated by this approach should—in conjunction with the measured mean Δc of mouse chromaffin granules (≈ 1.3 fF)—allow one to estimate a possible contribution of vesicles other than chromaffin granules to the fast secretory component.

Analysis of fluctuations among whole-cell ionic currents, which are observed during repetitive stimulation, has been frequently used to investigate properties of single ion channels (reviewed in ref. 20, stationary case and ref. 21, nonstationary case). In analogy we analyzed trial-to-trial fluctuations in whole-cell membrane capacitance changes (ΔC_m) in response to repetitive depolarizations, to study the capacitance of single fusing vesicles (for a theoretical description see *Materials and Methods*). C_m was measured at high time resolution (1 kHz) before and after each depolarization. The actual ΔC_m was then calculated as the difference of C_m averages taken before and after the pulse. To keep track of the stimulus-independent noise of the measuring system each depolarization was accompanied by a C_m measurement preceding the stimulus and another one following it, which, except for the lack of the depolarization, used the same measuring configuration. Fig. 2*A* shows a typical example of such a "triplet" C_m measurement with the capacitance increase due to a depolarization displayed in-between two control measurements. Each of the triplet C_m measurements provided two control and one test ΔC_m values to the analysis. Both short (5 or 10 ms) and long (100 ms) depolarizations were applied in separate experiments at 0.1 or 0.2 Hz and 0.05 or 0.1 Hz, respectively. We attribute the stable C_m increment elicited by the depolarizing pulse to exocytosis. The rapidly decaying C_m transient (ΔC_t) of Fig. 2*A* probably resulted from gating charge movement of sodium channels (14) because ΔC_t is still observable in chromaffin cells when voltage-activated Ca^{2+} current and secretion are
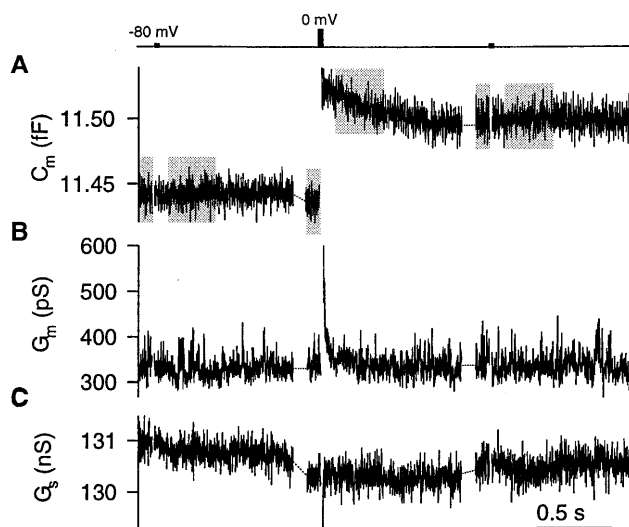

FIG. 2. Typical C_m measurement in chromaffin cells in slices. (*A*) Capacitance increase in response to a 10 ms long depolarization from the holding potential of -80 mV to 0 mV (center), which is flanked by preceding and after control measurements (no depolarization). After the depolarization the capacitance exhibits a decaying transient (ΔC_t) in addition to the stable elevation. The measuring sweeps were separated by 1–3 s (intervals indicated by dashed lines). The dc voltage protocol is displayed in the uppermost panel with the 10-ms constant voltage segments indicated by bold bars. Test and control ΔC_m values were estimated as the differences between C_m averages taken over the shaded time window after the constant voltage segments (long) with respect to averages over the preceding shaded window (short). (*B* and *C*) Membrane conductance (G_m) and series resistance (G_s) are shown to illustrate that there was no major crosstalk between C_m, G_m, and G_s lock-in estimates.
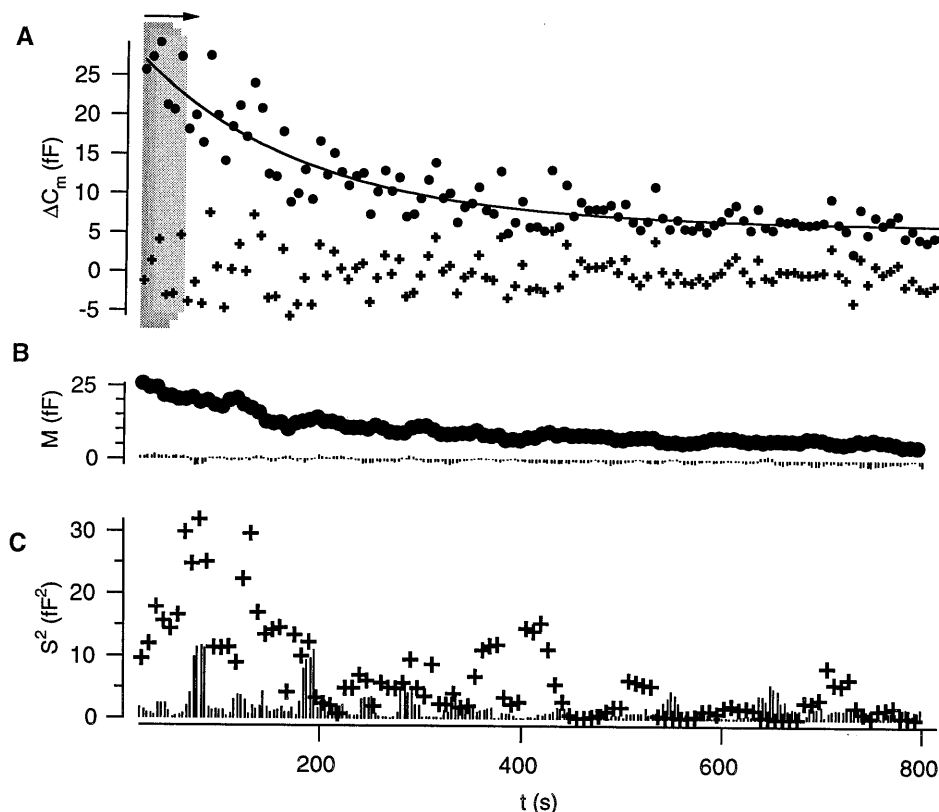
Fig. 3.   Application of nonstationary fluctuation analysis to test and control ΔC_m. (*A*) Test ΔC_m values, here measured in response to repetitive 10-ms depolarizations (control ΔC_m data not shown). The *x*-axis indicates the experimental time. The first two ΔC_m values were excluded (nonequilibrium conditions). An analysis bin of four (shaded boxes) was moved forward point by point to calculate sample (group) means and variances. Whereas test means were calculated from the "raw" ΔC_m values (circles) we measured test variances after subtracting a fit to the ΔC_m values (solid line, representing the secretory rundown) from the "raw" ΔC_m values (corrected ΔC_m values: crosses). This was done to avoid contaminating variance attributable to the trend. No such correction was performed for estimation of control variances. (*B*) The sample means for test (circles) and control (bars from zero) ΔC_m. (*C*) Test (crosses) and control (bars from zero) sample variances.

blocked, but is abolished by dibucaine (6, 14), which immobilizes sodium channel gating charges (22).

Because of rundown of the secretory response during the course of the whole-cell experiments only an analysis bin of four or eight neighboring ΔC_m values could be used. It was moved forward point by point to calculate means and variances, respectively. Fig. 3 illustrates the moving bin analysis of the ΔC_m data for a typical experiment (10-ms long depolarizations). In Fig. 3*A* each point represents a test ΔC_m from one triplet, and four values were used for calculating sample means (Fig. 3*B*, circles) and variances (Fig. 3*C*, crosses). The variation among test ΔC_m was largest during the early experimental time (high release probability) and dropped with decreasing ΔC_m amplitude. From Fig. 3 it is also evident that the means of the control ΔC_m (Fig. 3*B*, lines from zero) scattered around zero and that their variances (Fig. 3*C*, lines from zero) were similar to those of test ΔC_m only after secretory rundown. The variance between points of the fitted trend function (solid line in Fig. 3*A*, same total number of points) was calculated in groups as for the ΔC_m values to estimate the contribution of the trend in the data. It usually did not exceed 20% of the variance among the ΔC_m values. Nevertheless, we eliminated the impact of this trend by estimating the mean vesicular Δc from the variance of the difference between the experimental ΔC_m values and the fit (crosses in Fig. 3*A*).

Fig. 4 shows the plots of the trend-corrected variances versus means obtained from the same experiment as in Fig. 3 with $n = 4$ (Fig. 4*A*) and $n = 8$ (Fig. 4*B*) ΔC_m values. The positive correlation between variances and means for test ΔC_m can be regarded as evidence that the macroscopic whole-cell capacitance changes result from fusion of discrete vesicles (quanta).

The correlation was stronger when larger analysis bins were used. In 12 cells stimulated by short depolarizations the average slope of the regression line was 1.28 ± 0.16 fF for a bin of $n = 4$. For the 100-ms long depolarizations we obtained an average slope of the regression line of 1.39 ± 0.24 fF for a bin of four ΔC_m values (six cells, for an example see Fig. 4*C*). The difference between both means was statistically not significant. Therefore, we assume that both short and long pulses recruit the same vesicle population.

DISCUSSION

We have studied fluctuations between C_m changes evoked by repetitive depolarization and demonstrate that trial-to-trial variances and means obtained at different release probabilities are positively correlated. At least two questions have to be discussed before conclusions about the mean capacitance of fusing vesicles (Δc) can be drawn from these data:

What are sources for fluctuations among the ΔC_m values and what is their impact on the Δc estimation?

Is it reasonable to assume a Poisson distribution for the number of vesicles released per stimulus? In other words, does the slope of the relation of trial to trial variances to their corresponding means represent Δc, the quantal size?

Possible sources for ΔC_m fluctuation include: (*i*) sources with little stimulus-dependence (e.g., measuring system and spontaneous release), (*ii*) the nonsecretory artifact ΔC_t, and (*iii*) fluctuations attributable to stimulus-dependent membrane turnover (exocytosis and endocytosis).

The variance contributed by the measuring system and the spontaneous release was monitored by the control ΔC_m. It
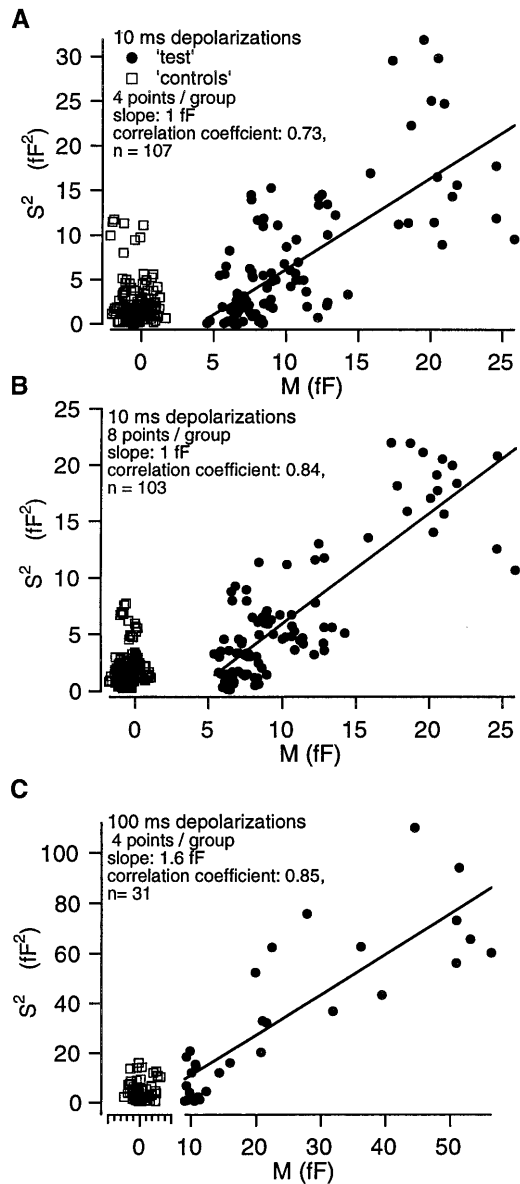
FIG. 4. Sample variances and means obtained for test ΔC_m are positively correlated. (*A*) A plot of the trend-corrected sample variances versus their corresponding means shown in Fig. 3 (10-ms depolarizations, bin-size = 4). Both measures were correlated for test ΔC_m (circles). The regression line had a slope of ≈ 1.0 fF. There was no correlation between variances and means in the case of control ΔC_m (squares). (*B*) Sample variances (trend-corrected) and means calculated from the same ΔC_m data with an analysis bin-size of 8. The larger bin slightly reduced the scatter, but again yielded a slope of the regression line of ≈ 1.0 fF. (*C*) An analogous plot for the analysis of an experiment where 100-ms depolarizations were repetitively applied (bin-size = 4, symbols as used above). The slope of the regression line fitted to the test data was 1.6 fF.

usually did not exceed 10 fF^2. Because it did not show trends comparable to those of the test data, we decided not to subtract it from the test variance but instead to document the control variance in Figs. 3 and 4 together with the latter. Most often, at late experimental times, the variances of the control ΔC_m and of the test ΔC_m were similar, whereas the means differed.

We believe that the test ΔC_m at late experimental times were dominated by a nonsecretory C_m artifact (ΔC_t, second source), which showed only little variation. ΔC_t probably results from gating charge movement of sodium channels (6, 14). In two cells, which had nearly no Ca^{2+} current and no secretion, but displayed large sodium currents, both the mean and the

variance of ΔC_m were essentially constant over the course of the experiments. This indicates that the ΔC_t contribution to ΔC_m does not largely change with time. In this case an unbiased Δc can be obtained if variances and means are measured over a range of release probabilities, as was done in the present study (see *Materials and Methods*, Figs. 3 and 4).

The measured random variable is the increase of C_m in response to identical, repetitive depolarizations. After evaluating the contributions of the measuring system and ΔC_t, we now discuss the fluctuations attributable to stimulus-dependent membrane turnover. We do not have evidence for a fast membrane retrieval process (endocytosis) in our whole-cell recordings from mouse chromaffin cells in slices (6), and slow retrieval would influence our results only minimally. Therefore, most likely the membrane surface area changes are determined by the number of fused vesicles in response to a given depolarization. In current models of secretion it is assumed that the secretory vesicles travel between certain vesicle pools (23, 24). After entering a readily releasable pool vesicles are exocytosed after an elevation of [Ca^{2+}] at their release sites. The number of fused vesicles is often modeled as the product of the number of readily releasable vesicles and a Ca^{2+}-dependent release probability. In that framework the random process we are considering is characterized by two probabilities: p, the probability of a fusion-competent vesicle to be released during a given stimulus and r, the probability of a given vesicle to be in the release-ready pool. It can be shown that release is indistinguishable from a Poisson process as long as the individual events are independent and $p \times r \ll 1$. Then the above analysis (Eqs. **2–5**) is valid with $\lambda = p \times r \times N$, where N is the total number of vesicles in both the reserve and the releasable pool (which is assumed to be large and constant for the time of an analysis window). As the analysis bin moves over the experiment λ drops in most experiments (see Fig. 3), which may be due to a decrease in any of the parameters p, r, and N. In the experiments with long depolarizations (see Fig. 4*C*) one would expect that p is close to 1 because 100-ms depolarization is much more than what is required to deplete the readily releasable pool in these cells (6). Nevertheless, we do not see a bell-shaped bending down of the variance versus mean relationship, as would be expected for a binomial-type process. This means that the product $p \times r$ is smaller than 1, in spite of $p \approx 1$, and it represents some indication that there is no statistical dependence between the processes of release and of replenishment of the release-ready pool. Binomial-type behavior would, for instance, be expected if there was statistical dependence in the sense that a vesicle has to be released from a finite number of release sites before other vesicles can replenish. Our result is in line with amperometric experiments that showed that, at least for the chromaffin granules, the number of vesicles released per depolarization follows Poisson statistics (8), and we suggest that the slope of the relation of local variances to their corresponding means represents Δc.

So far, for simplicity, release of only one population of vesicles has been considered. Independent of whether release of SLMVs follows Poisson or binomial statistics, a participation of SLMVs should reduce the Δc estimate, because the smaller vesicles contribute little variance. Interestingly, a recent study argued for parallel release of chromaffin granules and SLMVs from pheochromocytoma cells during flash photolyis of caged Ca^{2+} (25). Our estimate of the mean vesicle capacitance as derived from fluctuation analysis (1.3×10^{-15} F) is in good agreement with the value for the mean chromaffin granule capacitance, which we estimated independently by a crosscorrelation between capacitance and amperometric signals (1.3×10^{-15} F). It is much larger than that expected for SLMVs (10^{-17} F). Still, it is smaller than the Δc values obtained in previous studies for isolated bovine chromaffin cells [2.5 fF (3) and 2.7 fF (4)]. One possible explanation for the relatively low value of fluctuation estimates could be a fractional con-

tribution of SLMVs to secretion from mouse chromaffin cells in slices. The relative contribution of two parallel Poisson distributed release processes (which both show rundown) to the secretory response can be calculated from the slope of the variance versus mean plot if the mean individual capacitances of the two types of released vesicles (Δc_1, Δc_2 with a ratio $\gamma = \Delta c_2/\Delta c_1$) are known. Differentiation of an equation similar to Eq. 5 but now considering two kinds of vesicles yields:

$$\frac{\delta\sigma^2{}_{\Delta C_m}}{\delta\langle\Delta C_m\rangle} = \Delta c_1 \frac{1 + \dfrac{b}{a}\gamma^2}{1 + \dfrac{b}{a}\gamma}, \qquad [8]$$

where a and b are the fractional contributions of the two kinds of vesicles. The term $(b/a)\gamma = \delta$ is an impact factor for the relative contribution of vesicles Δc_2 to ΔC_m. When the product $\gamma \times \delta$ is very small ($\Delta c_1 \gg \Delta c_2$) Eq. 8 can be further simplified to

$$\frac{\delta\sigma^2{}_{\Delta C_m}}{\delta\langle\Delta C_m\rangle} \approx \Delta c_1 \frac{1}{1+\delta}. \qquad [9]$$

If we consider Δc_1 as the mean capacitance of chromaffin granules in mouse chromaffin cells (1.3 fF; as estimated by our crosscorrelation) the similarity of

$$\frac{\delta\sigma^2{}_{\Delta C_m}}{\delta\langle\Delta C_m\rangle}$$

and Δc_1 indicates a very small δ. This means that the relative contribution of chromaffin granules to ΔC_m is larger than that of a postulated population of small vesicles. Although we cannot completely rule out some SLMVs release during depolarization in slices, we conclude that the observed exocytic capacitance increases in response to long as well as short depolarizations mainly represent fusion of chromaffin granules.

It should be noted that both our experimental Δc estimates are slight overestimates of the means of the actual distribution of capacitance stepsizes. In the case of the crosscorrelation analysis the reason for this is that larger granules may be somewhat overrepresented. In the case of the variance analysis the reason for the overestimation is the expected scatter of the distribution. Assuming that the actual distribution of capacitance step sizes is similar to that of $Q_{amp}{}^{2/3}$ we estimate this error to be 30%.

In summary, we have shown that whole-cell capacitance measurements can be used to assay the mean individual capacitance of fusing vesicles. This may be of importance for studies on secretion from cells that do not release oxidizable material. Moreover, when the Δc are known for the relevant vesicle types, a relative contribution of the different vesicle populations to the observed secretion can be calculated.

1. Henkel, A. W. & Almers (1996) *Curr. Opin. Neurobiol.* **6,** 350–357.
2. Matthews, G. (1996) *Curr. Opin. Neurobiol.* **6,** 358–364.
3. Neher, E. & Marty, A. (1982) *Proc. Natl. Acad. Sci. USA* **79,** 6712–6716.
4. Chow, R. H., Klingauf, J., Heinemann, C., Zucker, R. S. & Neher, E. (1996) *Neuron* **16,** 369–376.
5. Thomas-Reetz, A. C. & De Camilli, P. (1994) *FASEB J.* **8,** 209–216.
6. Moser, T. & Neher, E. (1997) *J. Neurosci.* **17,** 2314–2323.
7. Whightman, R. M., Jankowski, J. A., Kennedy, R. T., Kawagoe, K. T., Schroeder, T. J., Leszczyszyn, D. J., Near, J. A., Dilberto, E. J., Jr., & Viveros O. H. (1991) *Proc. Natl. Acad. Sci. USA* **88,** 10754–10758.
8. Chow, R. H., von Rüden, L. & Neher, E. (1992) *Nature (London)* **356,** 60–63.
9. Annaert, W. G., Backer, A. C., Jacob, W. A. & de Potter, W. P. (1993) *J. Neurochem.* **60,** 1746–1754.
10. Sakmann, B. & Stuart, G. (1995) in *Single Channel Recording*, eds. Sakmann, B. & Neher, E. (Plenum, New York), 2nd Ed., pp. 199–211.
11. Hamill, O. P., Marty, A., Neher, E., Sakmann, B. & Sigworth, F. (1981) *Pflügers. Arch.* **391,** 85–100.
12. Schulte, A. & Chow, R. H. (1996) *Anal. Chem.* **68,** 3054–3058.
13. Sigworth, F. J. (1980) *J. Physiol. (London)* **307,** 97–129.
14. Horrigan, F. T. & Bookman, R. J. (1994) *Neuron* **13,** 1119–1129.
15. Augustine, G. J. & Neher, E. (1992) *J. Physiol. (London)* **450,** 247–271.
16. Burgoyne, R. D. (1995) *Pflügers. Arch.* **430,** 213–219.
17. Bruns, D. & Jahn, R. (1995) *Nature (London)* **377,** 62–65.
18. Chen, G., Gavin, P. F., Luo, G. & Ewing, A. G. (1995) *J. Neurosci.* **15,** 7747–7755.
19. Coupland, R. E. (1968) *Nature (London)* **217,** 384–388.
20. Neher, E. & Stevens, C. F. (1977) *Annu. Rev. Biophys. Bioenerg.* **6,** 345–381.
21. Heinemann, S. H. & Conti, F. (1992) *Methods Enzymol.* **207,** 131–148.
22. Gilly, W. F. & Armstrong, C. M. (1980) *Biophys. J.* **29,** 485–492.
23. Thomas, P., Wong, J. G., Lee, A. & Almers. W. (1993) *Neuron* **11,** 93–104.
24. Heinemann, C., Chow, R. H., Neher, E. & Zucker, R. S. (1994) *Biophys. J.* **67,** 2546–2557.
25. Kasai, H., Takagi, H., Ninomiya, Y, Kishimoto, T., Ito, K., Yoshioka, T. & Miyashita, Y. (1996) *J. Physiol. (London)* **496,** 53–65.